The U.S. National Lightning Detection Network™ and Applications of Cloud-to-Ground Lightning Data by Electric Power Utilities

Kenneth L. Cummins, E. Philip Krider, and Mark D. Malone, *Member, IEEE*

***Abstract*—Lightning is a significant cause of interruptions or damage in almost every electrical or electronic system that is exposed to thunderstorms. The problem is particularly severe for electric power utilities that have exposed assets covering large areas. Here, we summarize the basic properties of cloud-to-ground (CG) lightning, the primary hazard to structures on the ground, and then we discuss methods of detecting and locating such discharges. We describe the U.S. National Lightning Detection Network™ (NLDN), a system that senses the electromagnetic fields that are radiated by individual return strokes in CG flashes. This network provides data on the time of such strokes, their location and polarity and an estimate of the peak current. We discuss the network detection efficiency and location accuracy and some of the limitations that are inherent in any detection system that operates with a finite number of sensors with fixed trigger thresholds. We also discuss how NLDN data have benefited utilities by providing lightning warnings in real time and information on whether CG strokes are the cause of faults, documenting the response of fixed assets that are exposed to lightning, and quantifying the effectiveness of lightning protection systems. We conclude with some general observations on the use of lightning data by power utilities and we provide some guidelines on the uncertainties in lightning parameters that are acceptable in the industry.**

***Index Terms*—Fault diagnosis, fault location, lightning, lightning detection, power system lightning efects, remote sensing.**

I. Introduction

CLOUD-TO-GROUND (CG) lightning is the single largest cause of transients, faults, and outages in electric power transmission and distribution systems in lightning-prone areas. Additionally, lightning is a major cause of electromagnetic interference that can affect all electronic systems. The telecommunications industry suffers from both of these problems and must also deal with direct lightning strikes to facilities and communications infrastructure. In order to quantify and ameliorate the lightning hazard, the Electric Power Research Institute (EPRI) has sponsored the installation and development of the U.S. National Lightning Detection Network™ (NLDN), a system that now provides accurate data on the time, location, amplitude, and polarity of the individual return strokes in CG flashes. Real-time data from this network are also used by the U.S. Federal Aviation Administration, the National Weather Service, the Bureau of Land Management, and the Forest Service to determine the location, intensity, and movement of thunderstorms and the locations of lightning-caused fires. Archived lightning data are also being used in many areas of geophysical research and in forensic and insurance applications.

In this paper, we briefly review the components of cloud-to-ground lightning, the methods that are used to detect and locate lightning, the NLDN as it is presently implemented, the data that are provided by the network, and its salient performance parameters. We also describe some recent applications of lightning data by electric power utilities that utilize both real-time and archived data sets and we provide some general guidelines for the use of such data by utilities. We conclude with some plans for the future.

Manuscript received April 7, 1998; revised August 24, 1998.

K. L. Cummins and M. D. Malone are with Global Atmospherics, Inc., Tucson, AZ 85706 USA.

E. P. Krider is with the Institute of Atmospheric Physics, University of Arizona, Tucson, AZ 85721 USA.

Publisher Item Identifier S 0018-9375(98)09148-0.

II. Cloud-to-Ground Lightning

In order to introduce the terminology that we will use in discussing lightning and the NLDN, we will briefly review the luminous development of a typical CG discharge or *flash* and some of its characteristics. For further details about these processes, the reader is referred to [1]–[4].

A. Cloud-to-Ground Flashes

The majority of CG flashes begin with an intracloud (IC) discharge that is called the *preliminary breakdown*. After about a tenth of a second, the *stepped-leader* appears below cloud base and propagates downward in a series of intermittent steps. Most leaders effectively deposit negative charge along the leader channel; however, a few percent of leaders are positive. After a few tens of milliseconds, when the tip of the leader gets to within several tens of meters above ground, the electric field under the tip becomes large enough to initiate one or more upward *connecting discharges*, usually from the tallest object(s) in the vicinity of the leader. When an upward discharge contacts the leader, the first *return stroke* begins. The return stroke is basically an intense positive wave of ionization that propagates upward and discharges the leader channel at about half the speed of light. After a pause of 40–80 ms, another leader—the *dart-leader*—may propagate down the previous return-stroke channel and initiate a *subsequent return stroke*. A typical CG flash contains several strokes and lasts about half a second. In roughly 30–50% of all flashes to

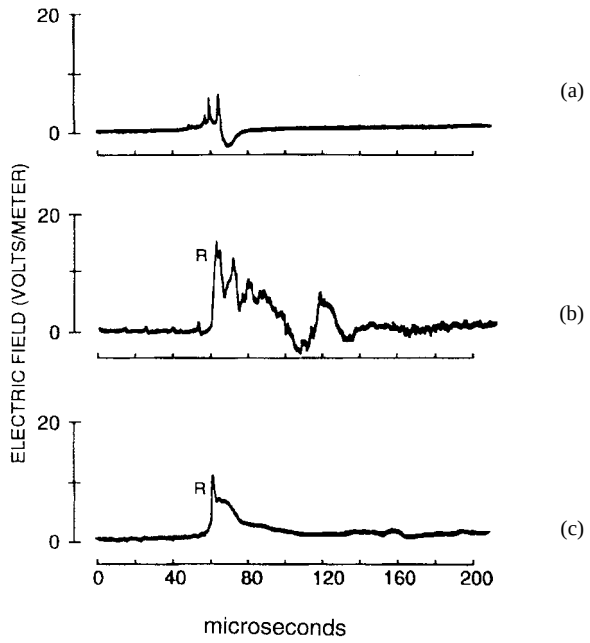

Fig. 1. Three of the many electric field impulses that were radiated by a CG flash at a distance of about 60 km. (a) Trace is from the preliminary breakdown within the cloud. (b) Trace is from the first return stroke. (c) Trace is from a return stroke subsequent to the first. (Adapted from [27].)

ground, the dart-leader propagates down just a portion of the previous return-stroke channel and then forges a different path to ground. In these cases, the flash actually strikes ground in two (or more) places.

Return stroke currents have been measured during direct strikes to instrumented towers and in rocket-triggered lightning [5]–[7]. The current in first strokes typically rises to a peak of 20 to 40 kA within a few microseconds, and the maximum rate of rise during this initial onset can be 100 kA/μs or more [8], [9]. The current falls to half peak value in about 50 μs and, following this, many strokes have a continuing current of hundreds of amperes or more for tens of milliseconds or more after the peak. A typical flash effectively lowers tens of Coulombs of negative charge to ground. Positive CG flashes, although less frequent than the negative, tend to produce larger peak currents and frequently transfer hundreds of Coulombs to ground.

B. Electromagnetic Fields

The electric and magnetic fields that are radiated by different lightning processes have characteristic signatures that are reproduced from flash to flash [3], [10]. For example, Fig. 1 shows three of the many impulses that were radiated by one CG flash at a distance of about 60 km. These particular signatures were recorded using a broad-band antenna system covering frequencies from about 1 kHz to 1 MHz in conjunction with a transient waveform digitizer with a "pretrigger" recording capability. Trace (a) shows a pulse that was radiated by the preliminary breakdown process within the cloud [11], trace (b) shows the waveform radiated by the first return stroke [10], and trace (c) shows a subsequent return-stroke. The small pulses that precede the first return stroke in Fig. 1(b) were produced by the final steps of the stepped leader, just before the onset of the connecting discharge and the return stroke [12]. Return strokes radiate efficiently at frequencies of a few to a few tens of kilohertz and are the largest source of atmospheric radio noise (termed atmospherics, spherics, or sferics) at these frequencies. At higher frequencies, the dominant sources of radiation are not return strokes, but rather breakdown processes within the cloud and the stepped-leader (see Section III-C). (See also [13] and [14] for a discussion of the sources and characteristics of atmospheric radio noise over the entire spectrum.)

Uman and others have developed models that describe the shapes of the electric and magnetic fields that are produced by return strokes at different distances [15]–[20]. The goal of much of this work has been to understand better how lightning transients couple to electric power systems. Most models predict that during the initial onset of a return stroke, i.e., up to the time of the initial peak current, the waveform of the distant (radiation) field can be approximated by the simple "transmission line model" [18],

$$E_{\mathrm{RAD}}(t) = -\frac{\mu_0 v I(t - D/c)}{2\pi D} \tag{1}$$

where E is the vertical electric field on the ground (assumed perfectly conducting) at time t, μ_0 the permeability of free-space, v the upward velocity of the stroke (assumed constant) near the ground, I the current at the base of the channel, c the speed of light, and D the horizontal distance to the flash [15]. (Note: An upward propagating, positive current produces a downward directed electric field). This finding suggests that the peak current in a return stroke can be estimated from a remote measurement of the electric and/or magnetic field if the source location and the stroke velocity are known and if the sensors have sufficient bandwidth to measure the peak field without distortion (also see Section IV-F below). For example, a typical first stroke produces a peak electric field of 5–10 V m^{-1} at a distance of 100 km [16]; now, assuming that the stroke velocity is about 1.5×10^8 m s^{-1} near the ground [21] and the peak field is 8 V m^{-1}, (1) predicts a peak current of 27 kA, a value that is in good agreement with tower measurements. A peak field of 8 V m^{-1} at 100 km also indicates that the stroke radiates more than 10 000 MW of peak power into the hemisphere above ground for the few microseconds near the peak [22].

The simple model expressed in (1) assumes propagation over a perfect, flat, conducting surface. In cases where fields are measured at distances of hundreds of kilometers, this assumption is not adequate. These propagation effects are discussed in greater detail in Section IV.F.

III. Lightning Detection Systems

We will now review some recent advances in instrumentation that can be used to detect and locate intracloud (IC) and CG lightning. Before the development of weather radars, a variety of sferics detection systems were the primary means of identifying and mapping thunderstorms at medium and long ranges [23]. In the 1920's, Watson–Watt and Herd [24]

developed a cathoderay direction finder (CRDF) that utilized a pair of orthogonal loop antennas tuned to a frequency near 10 kHz (where propagation in the earth-ionosphere waveguide is relatively efficient) to detect the horizontal magnetic field produced by lightning. The azimuth angle to the discharge was obtained by displaying the north–south and east–west antenna outputs simultaneously on an x-y oscilloscope, so that the resulting vector pointed in the direction of the discharge [25]. Two or more CRDF's at known positions were sufficient to determine the location of a discharge from the intersection of simultaneous direction vectors. Various low-frequency CRDF systems were used up to and during World War II in many regions of the world.

A. Gated Wide-Band Magnetic Direction Finders (DF's)

In 1976, an improved magnetic DF system was developed for locating CG lightning within a range of about 500 km [26], [27]. This system operated in the time-domain (i.e., covering the LF and VLF bands from about 1 to 500 kHz) and was designed to respond to field waveforms that were characteristic of the return strokes in CG flashes (see [27]). When such a field was detected, the magnetic direction was sampled just at the time of the initial field peak so that the direction vector pointed as closely as possible to the onset of the stroke and to the place where the stroke struck ground. The electric field was also sampled at this time to determine the stroke polarity. When employed in a network of DF's, the location of the stroke could be determined by triangulation, and the peak current could be estimated from the measured peak field [see (1)].

B. Time-of-Arrival (ToA) Sensors

Lewis *et al*. [28] have described a method for locating lightning that is based on measurements of the time-of-arrival (ToA) of a radio pulse at several stations that are precisely synchronized. Since radio signals propagate close to the speed of light, a constant difference in the arrival time at two stations defines a hyperbola and multiple stations provide multiple hyperbolas whose intersections define a source location. ToA methods can provide accurate locations at long ranges [29] and, if the antennas are properly sited, the systematic errors are minimal. Casper and Bent [30] have developed a wide-band ToA receiver [lightning position and tracking system (LPATS)] that is suitable for locating lightning sources at medium and long ranges using the hyperbolic method [31].

Networks of gated wide-band magnetic DF's and LPATS sensors have been operating in many countries for many years. (See [32] for a summary of the recent developments of lightning detection systems and their applications.) In [32. ch. 4] we will see that the NLDN utilizes a combination of DF and ToA sensing methods that are similar to those described in Sections III-A and B.

C. ToA Methods Operating at Higher Frequencies

The RF noise that is radiated by lightning in the high-frequency (HF) and very high-frequency (VHF) bands appears in bursts and within each of these bursts there are hundreds to thousands of separate impulses. Proctor [33] showed that when the difference in the ToA of each RF pulse is measured at four stations that are precisely synchronized, the locations of the sources can be mapped in three dimensions and the geometrical development of a burst can be traced as a function of time. Unfortunately, the physical processes that produce HF and VHF emissions in lightning are still not well understood. Proctor [34] noted that most bursts are characterized by a regular progression of source points and, therefore, he suggested that the RF sources were processes that create new ionization and extensions of old channels. When the location of each RF pulse within a burst was plotted, the width of the associated "radio image" ranged from about 100 m to 1 km [34]–[36]. The geometrical forms of intracloud discharges range from concentrated "knots" or "stars" a few kilometers in diameter to extensive branched patterns up to 90 km in length.

In recent years, the NASA Kennedy Space Center has developed a lightning detection and ranging system (LDAR) that is capable of providing three-dimensional locations of more than a thousand RF pulses within each lightning flash [37], [38]. This system is similar to that of Proctor, but the data acquisition is automatic, and the data displays are generated in real time (see also [39]). Today it is clear that high-frequency ToA methods offer great promise both for early warnings and for research, particularly in local regions and for those phases of the discharge that occur within the cloud.

D. Interferometric Methods

Hayenga and Warwick [40] showed that a radio interferometer could be used to measure the azimuth and elevation angles of lightning sources at VHF frequencies. Rhodes *et al*. [41] and Shao *et al*. [42] have developed this technique further and have used single-station interferometers to improve our understanding of the development of both IC and CG lightning.

Richard *et al*. [43], [44] have developed multiple-station networks of interferometers that can locate and map the sources of VHF radiation in two- or three dimensions with a time-resolution approaching 10 μs. A simple version of this system is available commercially and is reported to locate both IC and CG flashes [45], [46].

The physics of radio propagation over the spherical earth constrains sensors that operate primarily in the HF or VHF bands to have a short operating range relative to those that operate in the LF and VLF bands. This factor, when combined with the desire of power utilities to know precisely where each return stroke in each flash strikes ground and to have an estimate of the peak current (see Section VI below), has led the developers of the NLDN to utilize a combination of gated wide-band DF and ToA sensing methods, as discussed in Section III.A and B.

IV. The U.S. National Lightning Detection Network™ (NLDN)

The NLDN covers a total land area of about four million square miles (10 million km^2) that includes coastal regions and hills, flat agricultural lands in the central U.S., and extensive mountain ranges in western states that include peaks above 14 000 feet (4300 m). The electrical conductivity ranges from

Fig. 2. The locations of lightning sensors in the NLDN: triangles show IMPACT sensors and the circles show LPATS sensors. (Adapted from [47].)

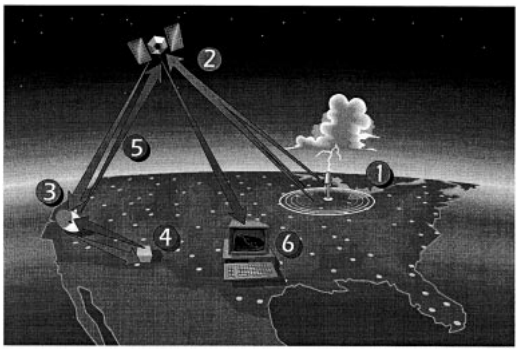

Fig. 3. Schematic diagram showing the NLDN data flow. Each sensor broadcasts lightning measurements to a satellite data acquisition system. All sensor data are processed in Tucson, AZ, and then data on the flash time, location, polarity, multiplicity, and peak current are rebroadcasted to users by satellite in near real time. (Adapted from [47].)

less than 1 to above 30 ms/m. Climate in the coverage area ranges from arid desert in the southwest to subtropical lowlands in the southeast to temperate rain forest in the northwest. The average annual lightning ground flash densities range from about 0.1 flashes/km^2/year near the West Coast to more than 20 flashes/km^2/year in portions of the Florida peninsula.

The historical evolution of the NLDN, some recent changes and improvements, and the salient performance characteristics have been discussed recently by Cummins *et al*. [47]. Basically, the NLDN began about ten years ago when data from networks covering the western United States [27] and the Midwest [48] were merged with data from a network covering the eastern United States [49], [50]. Real-time operation of the combined network began in 1989 [51], [52]. The sensors in the original NLDN were gated wide-band magnetic direction finders (DF's) of the type described by [26], [27], which were manufactured by Lightning Location and Protection, Inc. (LLP). In the late 1980's, a network of LPATS sensors manufactured by Atmospheric Research Systems, Inc. (ARSI) was also installed nationwide [53], [30]. By 1991, there was sufficient commercial interest in national scale lightning information to justify the establishment of a commercial data service company. To meet this need, LLP and the Electric Power Research Institute (EPRI) formed Geomet Data Services, Inc. (GDS) and today, GDS, LLP, and ARSI have been combined to form Global Atmospherics, Inc. (GAI), a wholly owned subsidiary of the Sankosha Corporation.

A. Sensors

In 1995, the original DF sensors employed in the NLDN were upgraded to include GPS pulse timing data in addition to the magnetic direction and signal amplitude; these sensors are now known by the trade name IMPACT. The NLDN currently contains 47 IMPACT sensors and 59 upgraded LPATS-III sensors from the original ARSI national network; their locations are shown in Fig. 2. For operation in the NLDN, the standard gain of the IMPACT sensors was increased, the trigger threshold was reduced, and the waveform acceptance criteria were altered to allow the detection of lightning beyond 500 km. Waveform selection criteria were also added to the LPATS-III sensors so that nearby cloud discharges and leader pulses would not trigger these systems.

B. Data Acquisition

A sketch of the NLDN and data flow is shown in Fig. 3. The ground-based sensors transmit lightning data $\{1\}$ to the Network Control Center (NCC) in Tucson, AZ, via a two-way satellite communication system $\{2-3\}$. Data from the remote sensors are recorded and then processed in the NCC $\{4\}$ to provide the time, location, and an estimate of the peak current in each return stroke in real time. The real-time data are then sent back out the communications network for satellite broadcast dissemination $\{5\}$ to real-time users $\{6\}$. All this takes place within 30–40 s of each lightning flash. This delay consists of a fixed, 30 s hold time and a variable processing and communications delay. Only CG flash data with 0.1-s time resolution are distributed via the satellite broadcast link. Higher resolution flash and stroke data are available over other communications links. All recorded data are reprocessed off line within a few days of acquisition and then stored in a permanent database that can be accessed by users who do not require real-time information. Since 1991, the NCC and real-time data delivery system have been on line more than 99.5% of the time.

C. Errors in Real-Time Data

The real-time NLDN data may contain several errors that are subsequently eliminated by the reprocessing off line. For example, systematic errors in the magnetic directions or "DF site errors" can be identified and corrected after sufficient lightning data have been accumulated (typically after one to three months of operation) [48], [54], [55]. Similar corrections can be derived for the gain of a sensor. Prior to applying such corrections, however, the information from any uncorrected or uncalibrated sensor(s) must be ignored or deemphasized so that the response of the sensor under test can be determined. Once the correction factors have been determined, all the NLDN data are then reprocessed and stored in the permanent data archive.

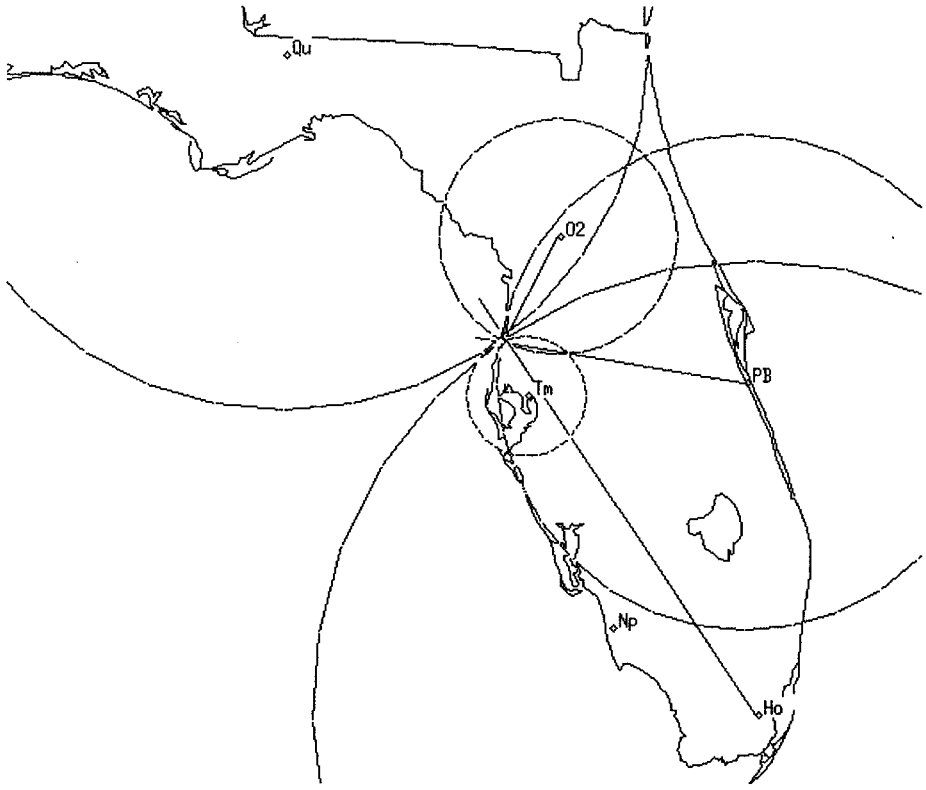

Fig. 4. Example of a return stroke that was located by two LPATS sensors (circles only) and three IMPACT sensors (circles and vectors). (Adapted from [47].)

The real-time NLDN data stream will not report events if there are delays in receipt of the sensor information due to rain fade or data congestion during periods of high data rates. Typically, congestion occurs when the lightning rate over the entire United States. exceeds 80 000 strokes per hour. In these situations, the missing strokes (typically 2–5%) are retrieved by reprocessing the recorded data off line.

D. Location Algorithm

The NLDN uses a least-squares optimization procedure to compute flash locations in real time [54], [56]. The optimum location (latitude, longitude) and onset time at the source are determined by finding the position on an oblate spheroidal earth that makes the unconstrained error function a minimum; the value of this function at the minimum describes the overall accuracy of the location. The error function includes both direction and time measurements weighted by a reciprocal of the expected errors. The accuracy of the stroke time is determined by the random errors in the measured ToA (and the associated propagation delays) and has a standard deviation of about 1.5 μs. The random errors in the direction measurements plus any residual site errors have a standard deviation of about 0.9°.

The combined MDF and ToA location algorithm offers many advantages over either a DF or ToA method taken alone. For example, a discharge that occurs along the baseline between two IMPACT sensors will be more accurately located by the intersection of two direction vectors and two range circles than by the direction intersection alone [56]. The location algorithm that is implemented in the NLDN allows arbitrary combinations of IMPACT (DF and ToA) and LPATS (ToA only) sensors to be used in the computation. Typically, strokes with an estimated peak current of 25 kA are detected by 6–8 sensors; 5-kA strokes are detected by 2–4 sensors; and 100-kA strokes are reported by 20 or more sensors.

Fig. 4 shows a typical lightning stroke in Florida that was detected by five NLDN sensors—three IMPACT and two LPATS-III sensors. The direction measurements are shown as straight-line vectors and the ToA measurements are represented by range circles centered on each sensor.

E. Flash Multiplicity and Polarity

The NLDN location algorithm groups strokes into flashes and determines the flash multiplicity and polarity. Prior to 1995, each DF sensor counted all strokes that occurred within 2.5° of the first stroke for a period of one second after the first stroke and the flash multiplicity was simply the largest number of strokes detected by any DF. This method tended to overestimate the true multiplicity when concurrent flashes occurred at similar azimuths relative to any of the sensors [47].

In the current NLDN algorithm, strokes are grouped into flashes using a spatial and temporal clustering algorithm that is illustrated in Fig. 5. Strokes are added to any active flash for a period of one second (the NLDN flash duration limit) after the first stroke as long as the additional strokes are within 10 km of the first stroke and the time interval from the previous stroke is less than 500 ms. In the unlikely event that a stroke is a candidate for more than one flash, it is

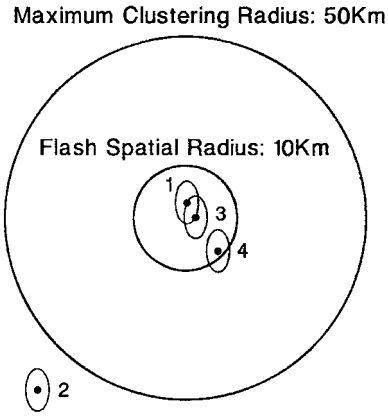

Fig. 5. Location-based flash grouping algorithm. Strokes 1, 3, and 4 constitute one flash; stroke 2 is regarded as a separate flash. (Adapted from [47].)

assigned to the flash with the closest first stroke. Additionally, if a stroke is located more than 10 km from the first stroke (and is within a 50-km clustering radius), but is not clearly separated from that stroke because their location confidence regions overlap (see Section V), then the stroke is included in the flash. The maximum multiplicity in the real-time data stream is 15 strokes; any strokes after that are considered the beginning of a new flash. Subsequent strokes are counted in the multiplicity even if they have a polarity that is opposite that of the first stroke. The real-time NLDN flash location is the location of the first return stroke and the flash polarity is the same as that of the first stroke.

F. Peak Current

The NLDN (like other wide-band systems that sample return stroke peaks) estimates the peak current in each return stroke (or flash) using the peak signal amplitudes that are measured at each sensor site. A range-normalized signal strength (RNSS) is then computed for each site by multiplying the measured signal by the range plus a correction for propagation over the finitely conducting ground [47]. The resulting calibrated RNSS is then averaged over all sensors that reported the event and converted to a current using an empirical fit, i.e., $I_{\text{peak}} = 0.185$ RNSS. For the NLDN, this formula has been derived by comparing the calibrated RNSS value to peak current measurements in rocket-triggered lightning [47], [57]. This method is equivalent to assuming that the peak radiated field is proportional to the peak current at the ground as in (1) and that return stroke velocities are equal and constant. It should be noted that the available data on rocket-triggered lightning are limited to negative subsequent strokes and that there are still no published "calibrations" of NLDN current estimates for natural first strokes of either polarity. The NLDN currents inferred for rocket-triggered subsequent strokes deviate from measurements by about 5 kA or 20–30%. Detailed tests of the simple transmission-line model also show similar deviations [58] (see also the discussions in [8] and [9]); therefore, the NLDN values of peak current should be viewed as approximations with an uncertainty of at least 20–30%. The peak current given in a real-time NLDN flash report is the peak current of the first return stroke at that location.

In addition to the calibration issues discussed above, there are two additional limitations that can seriously affect the accuracy of peak current estimates, particularly in small networks with few sensors. The first is that when a small number of sensors detect a stroke, then the uncertainty in the estimated RNSS at the source is large. For example, if only two to three sensors detect a stroke, the RNSS uncertainty is typically about 40% larger than when four to six sensors respond. The second limitation arises when different sensors measure fields that propagate over variable terrain with different propagation losses. In this case, the effect of the inclusion/exclusion of an individual sensor in a small network can dramatically change the average RNSS.

The broad coverage area of the NLDN provides a rich data set for studying how various lightning parameters depend on climate. For example, the median peak current for negative first strokes averaged for the three-year period of 1995–1997 ranges from 18 to 19 kA in central New York, to 23–24 kA in central Florida. These values are somewhat lower then the median value of 30 kA obtained by Berger [5] and the geometric mean value of 33 kA found by Garbagnati [6] for strikes to towers in Switzerland and northern Italy. There are many possible reasons for such differences including the effects of towers on the measurements and/or the details of the measuring systems. A detailed discussion of these factors is beyond the scope of this paper.

V. Network Performance Parameters

Over the past six years, the NLDN has undergone a series of upgrades and extensions that have provided substantial improvements in the overall network detection efficiency, location accuracy, event timing, and immunity to false reports [47]. It should be noted that all of these performance parameters are important in utility applications and that no measurement system is perfect. Because of the discrete nature of ground-based lightning detection networks, the detection efficiency and location accuracy will necessarily vary with position. Both of these parameters are functions of the source amplitude and could change abruptly if there are any outages in nearby sensors or the data communications subsystems. López *et al*. [59] have shown that even the motion of individual storms within a small regional network can seriously affect the apparent peak current distributions and the fractions of flashes that have positive polarity. These general issues are discussed below. In the NLDN, these problems are mitigated (at least in part) by its large size and its inherent redundancy.

A. Detection Efficiency

The ability of a network to detect CG lightning can be characterized by either a stroke or flash detection efficiency (DE), i.e., the fraction of the actual strokes or flashes that are detected and reported by the network. Typically, a sensor will fail to report a stroke if the peak field is below the trigger threshold or if the waveform fails to pass the return stroke selection criteria, i.e., the pretrigger, risetime, width,

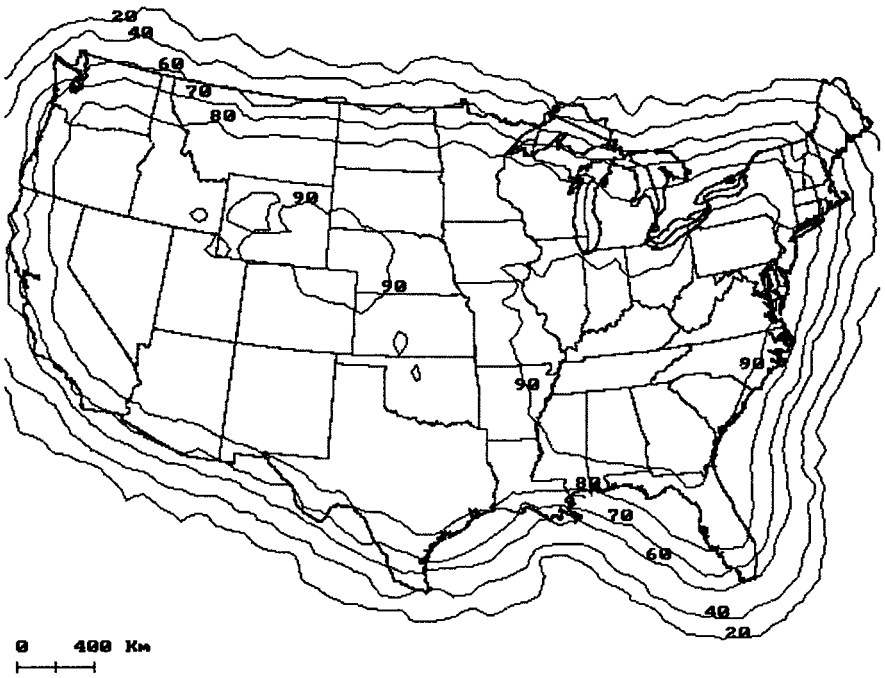

Fig. 6. NLDN flash detection efficiency (DE) computed using a measured source amplitude distribution. Contours show the cumulative values of DE in percent. (Adapted from [47].)

multiple-peak structure, and bipolar shape criteria that are applied to each waveform [27].

The spacing, gains, and threshold of the sensors are critical parameters in the design of reliable networks. If a network is designed such that the sensors are separated by more than their "nominal range," i.e., the distance at which small return strokes can no longer be detected, then the loss of communications or power at a single site can cause the network to miss a significant fraction of the events. The loss is largest in networks with a small number of sensors. The NLDN sensor spacing shown in Fig. 2 is set to be approximately 60–75% of the nominal range. This configuration was chosen so that 80–90% of the first strokes that produce a peak field of 1.0–1.5 V/m, range-normalized to 100 km or a peak current of about 5 kA or more will be detected. If the peak field (or current) is below this nominal value, the stroke might still be detected if it is close to two or more sensors; conversely, even a larger peak field (current) will not be detected if it is too far away from the sensors (outside the network). Because the fields radiated by first strokes tend to be larger than for subsequent strokes, the overall flash DE is assumed to be the same as that for first strokes. It should be noted that if the gain or threshold of the sensors in a network differ dramatically or are highly dependent on direction, then characterization of DE becomes very complex.

Fig. 6 shows an estimate of the NLDN detection efficiency for negative flashes that exhibit more than 5-kA peak current. These computations were done using an empirically derived source distribution, assuming that the range-normalized peak field is proportional to the peak current (see Section IV.F) and using a simple model for field propagation [47]. Note that the DE in Fig. 6 decreases rather rapidly with distance outside the perimeter of the network. Since return strokes that fail to pass the waveform selection criteria are not included in the source distribution, Fig. 6 should be viewed as the relative DE of the NLDN for waveforms that do pass the waveform criteria.

Idone *et al.* [60] have recently estimated the DE of the NLDN using television records of visible flashes near Albany, NY. These authors found that the absolute DE varied from storm to storm and was a strong function of the peak field (or current) in the strokes. The NLDN detected strokes with an estimated peak current greater than 16 kA with a DE of about 97% (38 out of 39); the DE was about 15% for strokes in the 6–10 kA range and zero for strokes below 6 kA. When a 5-kA threshold was applied to the DE computation (as in Fig. 6), Idone *et al.* found that the cumulative flash and stroke DE were 84% and 66%, respectively, values that are consistent with the estimates in Fig. 6. It should be noted that a 5-kA threshold is thought to include most (>95%) of all negative first strokes. However, it is possible that a significant fraction of subsequent strokes could have peak currents below this value.

We note also that the data summarized in Fig. 4 of Idone *et al.* [60] show that the number of return strokes that are rejected by the NLDN waveform selection criteria is quite small, at least in the New York test region (see preceding paragraph).

B. Location Accuracy

Random and systematic errors in the time and direction measurements will produce random and systematic errors in the source location and onset times. Hiscox *et al.* [54], Passi and López [55], and others have described methods for identifying and then correcting the systematic angle or "site errors" that frequently occur in magnetic direction measurements. The basic procedure is to search for a pattern in the residual errors (plotted as a function of angle) using an ensemble of lightning

Sec	Latitude	Longitude	Current_kA
34.9818730	35.5143	-80.3533	-38.626
35.200530	35.5138	-80.3411	-27.232
35.417380	35.4753	-80.4137	-39.312
35.521885	35.5156	-80.3442	-21.331
35.774949	35.4706	-80.4306	-10.064
35.926924	35.5189	-80.3441	-22.848
35.1717237	35.5134	-80.3395	-31.302
35.2695261	35.5045	-80.3501	-21.479

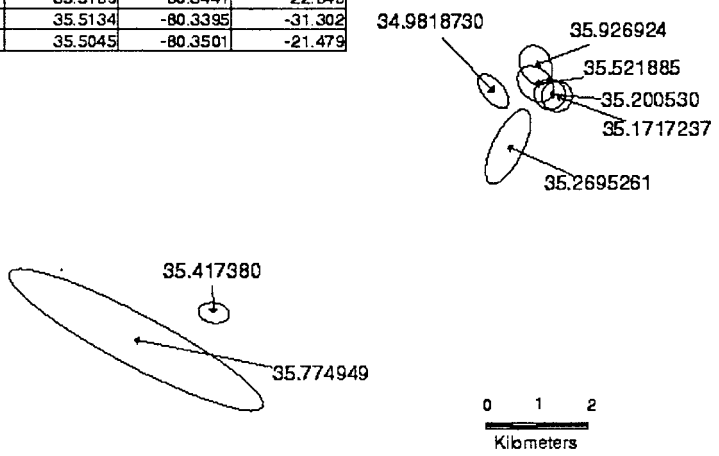

Fig. 7. The locations and 50% confidence regions for each return stroke in a multistroke CG flash. The table shows the sequence of strokes and their locations, the estimated peak current in kA and polarity, and the number of NLDN sensors that reported the stroke. Note that there were at least two different ground contact points—one to the Northeast and the second to the Southwest.

flashes that are uniformly distributed over the network and then to add angle corrections to these measurements that make the errors a minimum. Systematic errors are also present in the arrival time measurements due to propagation over complex terrain and variations in the conductivity of the surface. Currently, the NLDN location algorithm lumps such errors into the estimated random errors that are assigned to the arrival times.

We have previously noted that when DF and ToA data are combined into a common error function, the accuracy of the lightning location is enhanced. One way to quantify the effects of random (and uncorrected systematic) errors on the position is to give the spatial dimension of the associated confidence region for each stroke. If the errors are normally distributed, the confidence regions will be elliptical [61] and the location accuracy can be characterized by giving the length of the semi-major and semi-minor axes and the orientation of the error ellipse.

Fig. 7 shows examples of error ellipses that describe the 50% confidence regions for each return stroke in a typical CG flash. Note that the semi-major axes range from about 600 to 1200 m; typically, larger dimensions correspond to lower signal amplitudes and fewer sensors reporting the stroke. Note also that for this particular flash there appeared to be at least two different ground strike points separated by 7–9 km.

Fig. 8 shows computations of the median NLDN position error, i.e., the length of the semi-major axis of the 50% confidence region, assuming that the random errors in ToA have a standard deviation of 1.5 μs, that the random errors in direction are 0.9° and that the only sensors reporting are those within 550 km of the stroke (for details of this computation, see [47, Appendix A]). Note in Fig. 8, that the median accuracy of the NLDN is about 500 m over most of the continental United States.

Idone *et al*. [62] have evaluated the location accuracy of the NLDN near Albany, NY, by comparing the NLDN reports of individual strokes with locations derived from television records. These authors found that the accuracy of a stroke depended on the stroke amplitude (or the number of NLDN sensors that responded) and strokes with an estimated peak current of 20–40 kA were generally within 400–600 m of the locations computed from television records.

In [62], the authors were able to evaluate the location accuracy of 11 return strokes that terminated on three structures at precisely known locations. The NLDN locations exhibited a systematic shift of 300–400 m to the northeast that is probably due to residual site errors and small systematic errors in ToA. Errors in ToA can be produced by the effects of complex terrain on radio propagation and limitations in the present propagation model. Therefore, given the results of Idone *et al*. [62], it would be prudent to assume that a reasonable lower bound on both the semi-major and semi-minor axes of the median (50th percentile) confidence ellipse is in the range of 300–400 m.

C. Flash and Stroke Times

The flash time that is reported by the NLDN is the estimated time of onset of the first return stroke in the discharge. This time is derived in the optimization algorithm using the measured arrival times at each sensor after subtracting an interpolation to the source, i.e., the times required for the field to propagate from the source to the sensors is subtracted from the times that the sensors measured. As a point of interest, the onset time is very close to the onset of the current in the stroke, but it is typically several tens of milliseconds *after* the preliminary breakdown begins in the cloud, and it is typically several tenths of a second *before* the flash ends. Because the stroke time is a free parameter in the NLDN

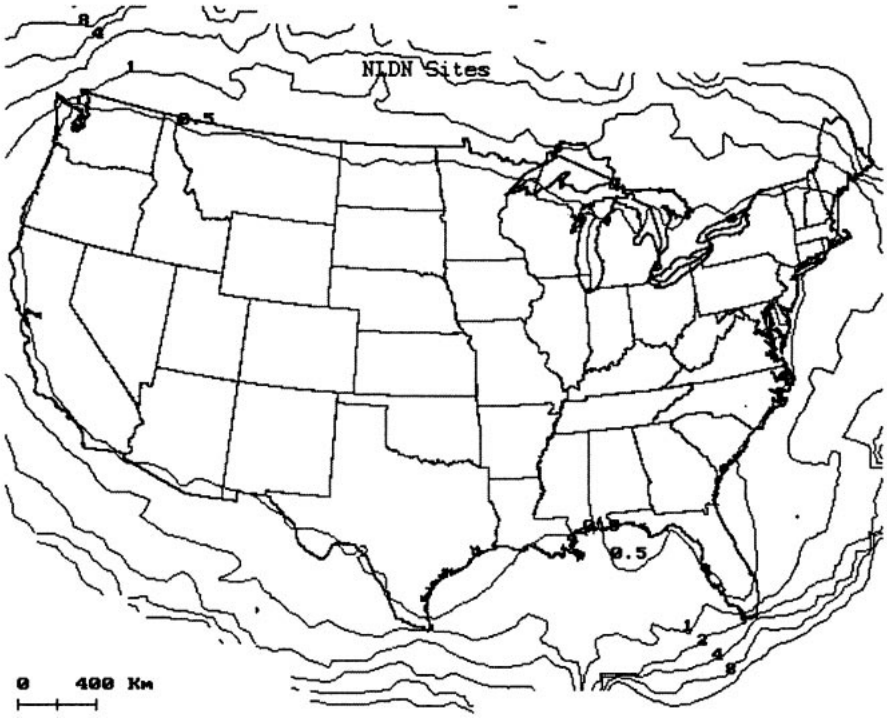

Fig. 8. Contours of the length (in kilometers) of the semi-major axis of the NLDN error ellipses. The values represent the median (50%) confidence level. (Adapted from [47].)

positioning algorithm and the source position is uncertain to within a few hundred meters, the onset time should be accurate to about 5 μs. A stroke time resolution of 5 μs is more than adequate to resolve separate return strokes within the flash and to determine which of these strokes might be correlated with a fault on a power line (see Section VII-C).

VI. Electric Utility Applications

In 1979, the Tampa Electric Company began using real-time lightning maps to monitor the approach of lightning storms, estimate their severity, and then preposition, hold over, or call out repair crews as necessary [63]. Today, more than 80 electric power utilities in the United States use real-time NLDN data in a similar fashion in their daily operations [64]–[67], and in conjunction with EPRI's Lightning Protection Design Workstation [68].

Real-time lightning data can also be combined with on-line monitoring of circuit breakers, relays, and/or substation alarms to improve operations and minimize damage. Typical practice is to clear nonpersistent faults (such as lightning) with an instantaneous circuit breaker or relay operation. During lightning storms, however, multiple strokes, improper relay reclosures, or temporary faults that persist for the duration of the breaker sequence can cause feeder lockouts. Such lockouts can be restored by reclosing the feeder breaker, but an important concern at the time of lockout is whether or not the fault is permanent or whether it was caused by lightning. The real-time lightning data provide this information, giving utilities a powerful tool both for averting damage to and speeding the restoration of their systems.

A. Area Flash Densities

It is common practice to characterize the overall lightning threat to a power system with maps of the area density of flashes. In the past, such estimates were derived from thunder-day and/or thunder-duration statistics compiled by the National Weather Service or more directly from readings of lightning flash counters. (For overviews of these methods, the reader can consult [2] and [69]–[71], and the references therein.) Clearly, a direct measurement of the CG strike locations provides a much better and more accurate method of quantifying the lightning exposure.

Fig. 9 shows a contour map of the annual area density of the first stroke in CG flashes over the United States derived from an average of NLDN data over the years 1989–1993. This plot was made by counting all flashes that occurred in 5-km^2 cells and then smoothing these counts by averaging over the eight "nearest neighbor" points. In making Fig. 9, the United States was divided into an 88 $\times$ 50 grid, each element (about 60 $\times$ 60 km^2) containing the total smoothed counts and contour lines were drawn as Bezier splines [71]. The measured flash density is not corrected for imperfect detection efficiency (see Section V-A). The inset of Vermont at the upper right shows the original high resolution (5 km^2) data and is included to illustrate the considerable detail that is missing in the lower resolution plot. The spatial smoothing required for the national map has reduced variations of a factor of eight over Vermont to an apparent factor of two. Note that the flash densities tend to be highest in the Southeast and lowest along the Pacific coast.

Maps like Fig. 9 can be used to estimate approximately how often powerlines will be exposed to nearby and direct strikes and to optimize expenditures when routing, protecting,

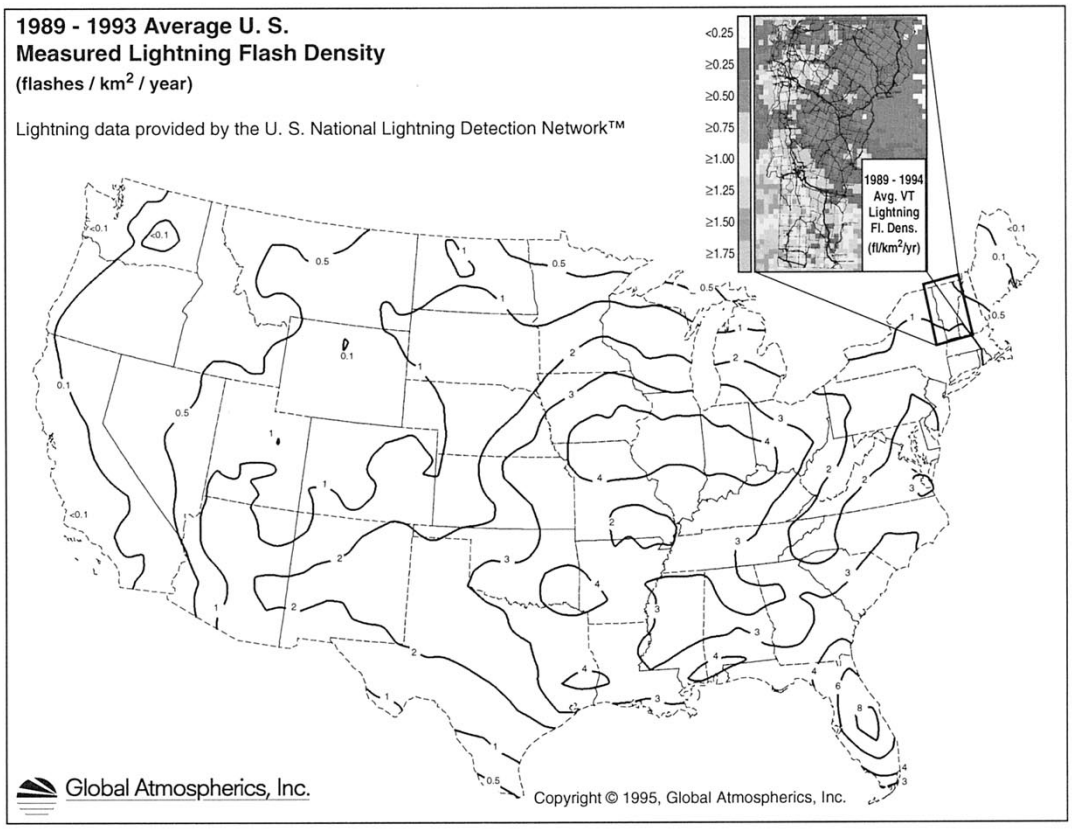

Fig. 9. The average annual area density of the first stroke in CG flashes (number per km^2 per year) measured over the United States from 1989 to 1993. The inset over Vermont illustrates the regional detail that is obscured in the low-resolution plot.

and/ or upgrading new or existing lines [72]. Higher resolution data are required for accurate estimates of the exposure of specific lines or line segments. EPRI [73] has developed a Lightning Protection Design Workstation (LPDW) to assist in such efforts and the LPDW uses archived NLDN data to quantify the local, regional, and national flash densities.

B. Fault Detection and Classification

Two relatively new applications of archived NLDN data are the classification of faults on transmission and distribution systems and the evaluation of the performance of various methods that are used in lightning protection. For both of the above, knowledge of the time, location, and peak current of each return stroke provides a valuable empirical database with which to address the key issues. We will now give some specific examples.

1) Minnesota Power and Light: Minnesota Power and Light (MPL) uses NLDN data to understand and quantify the performance of transmission systems that are exposed to lightning [74], [75]. Fig. 10 shows an "asset exposure map" of all CG strikes in 1995 in a region that contains a 32-mile 115-kV transmission line. Strokes within a distance of 2.5 km of the line are shown in bold; the number of these events characterizes the exposure of the line to nearby and direct lightning strikes in that year. By combining data such as these with estimates of the peak current and fault records, MPL has quantified the performance of individual lines and line segments on a per-strike basis and has evaluated where improvements in line protection or line design will be most cost effective [75].

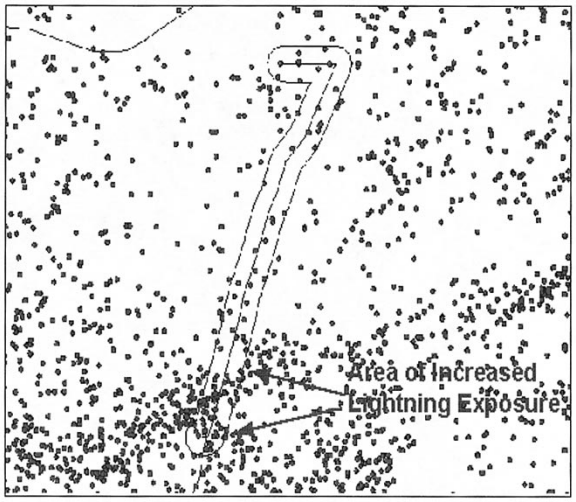

Fig. 10. A map of the CG strokes that struck in the region of a 32-mile 115-kV transmission line in 1995 in Minnesota. Note that in this year, there were two areas that had high exposure to lightning. The flashes plotted in bold were located within 2.5 km of the line. (Adapted from [74] and [75].)

Fig. 11 shows the locations of all strokes that caused faults on a 62-mile unshielded 115-kV line during 1994 and 1995. Note how the strokes (and faults) are concentrated in two areas

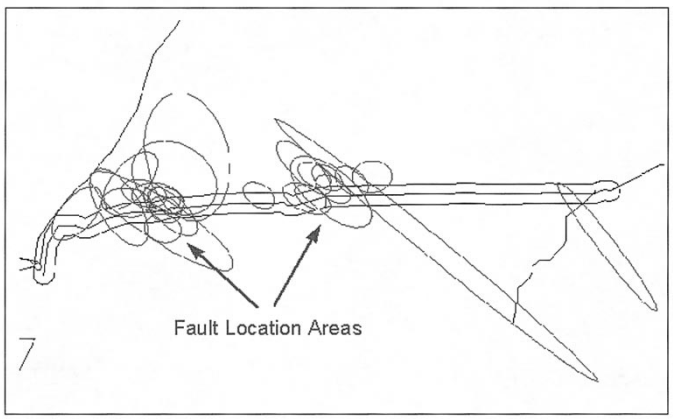

Fig. 11. The locations of all return strokes and the associated 50% confidence regions that were time correlated with faults on a 115-kV transmission line in Minnesota. Note that these strokes tend to cluster into two regions where the lightning protection was less effective than elsewhere. (Adapted from [74] and [75].)

about eight miles long. Since the lightning flash density or exposure was more or less uniform over the entire line, MPL could target their mitigation efforts primarily in the regions with faults rather than along the entire line [75]. The large confidence ellipses in Fig. 11 were obtained prior to a major upgrade of the NLDN in 1995; in these cases, precise timing of the faults (to the millisecond) was required to identify the particular stroke that caused the fault.

2) Georgia Power (GP): There is no question that lightning is the most important cause of faults and outages in the GP service area; however, sometimes faults are caused by factors other than lightning, even during severe thunderstorms. When faults are individually time-stamped to millisecond accuracy, NLDN data can be used "after the fact" to assess which faults were due to lightning and which were not.

An example of the latter occurred when there were two simultaneous outages on two nonadjacent 230-kV transmission lines [56]. NLDN data showed that a stroke with a negative peak current of 40 kA struck within 160 m of one line, but no lightning was detected anywhere near the other. Since both lines had tripped at the same time, the cause of the fault on the second line was investigated and later found to be due to an incorrect relay operation. Thus, the NLDN helped to identify a problem on the second line, namely that the relay tripped when there was an external fault on the first line. Prior to the existence of the NLDN, it would not have been possible to find a problem such as this.

3) Sacramento Municipal Utility District (SMUD): During 1995 and 1996, the Sacramento Municipal Utility District (SMUD) experienced 24 interruptions on a 230-kV transmission system, including lines at 69 kV and suspected that they might have been caused by lightning. Fig. 12 shows the geometry of the system and the NLDN flash densities measured in the service region in 1995 and 1996. (Note in Fig. 12 how the topography of the Sierra Nevada mountains to the east strongly influences the lightning densities.) Fig. 13 shows 233 lightning strokes that struck within 3.0 km of the lines, 130 in 1995, and 103 in 1996, and how they were distributed. Of the 24 faults previously suspected to be caused by lightning, 22 occurred in 1995 and two occurred in 1996. Since the actual exposure to lightning was approximately equal in both years and strikes occurred near most of the line, we can infer that lightning was probably NOT the cause of the faults in most instances. This supposition is supported by further analysis of the 24 candidate faults; namely, when the faults were time-correlated with NLDN strokes to within one minute, only four of the 24 showed a correlation. These strokes are plotted in Fig. 14 together with their 50% confidence regions. Strokes numbered 1–3 occurred near 69-kV lines and had low to average peak currents. Stroke 4 was near the 230 kV line and had a negative peak current that was larger than normal—about 45 kA. Of the 24 original candidates, only these four strokes probably caused a fault. The low-to-average estimated peak currents for strokes 1–3 suggests that there are lower levels of lightning protection in the areas where the ellipses intersect the line (see Fig. 14) even in light of the fact that there are lower insulation levels on a 69-kV line.

VII. Observations on the Use of Lightning Data by Power Utilities

In Section V, we have seen that the parameters that the NLDN reports for each lightning stroke or flash necessarily have some uncertainty. Anyone using data derived from the NLDN (or any other lightning locating system) should understand the limitations of the measuring network in order to avoid misinterpreting the data. Although a detailed discussion of this subject is beyond the scope of this paper, some of the key factors that affect electric power utilities are summarized below.

A. Detection Efficiency

In Section V-A, we saw that the NLDN DE can vary with location (due to network geometry) and with time (due to network status and possibly the nature of the thunderstorm). Because of this, care must be taken when interpreting changes in the numbers of strokes or flashes that are detected over various scales of space and/or time. In addition, any spatial or temporal variations in DE can also affect the measured peak current distributions and the fractions of the reports that have a positive polarity. The NLDN tries to maintain a uniform and high DE throughout the United States. DE computations (such as those shown in Fig. 6) can be used as a "first-order" estimate of the variations in DE with region although one must be careful near the "edges" of the network.

B. Location Accuracy

The location accuracy that is required depends on the specific application. For example, a location accuracy of 2–4 km is usually more than adequate for real-time storm tracking because the dimensions of a typical lightning cell are 10 km or more. Also, such applications rarely require data on individual strokes or precise timing. Similarly, when the asset exposure is computed over long time intervals, a 1–2-km location accuracy is usually sufficient. On the other hand, when analyzing transmission or high-voltage distribution line faults,

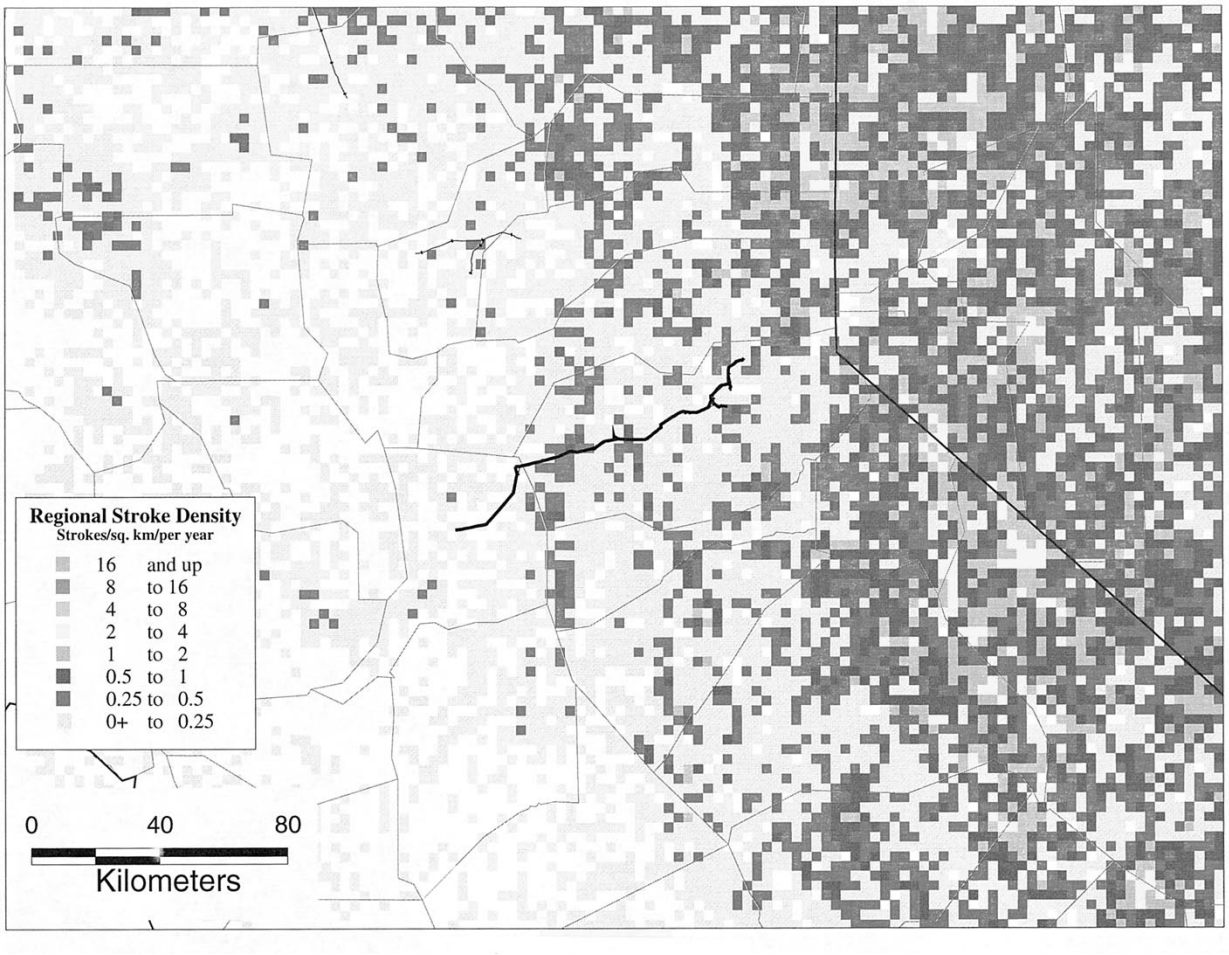

Fig. 12. A high-resolution flash density map in the region of the SMUD transmission line in California (1995–1996). Note the influence of the topography of the Sierra Nevada Mountains on the regional flash density.

the location accuracy must be good enough to insure that a particular lightning event is, in fact, associated with the line of interest. When analyzing faults that are time correlated with individual return strokes, the location accuracy should average 0.5 km or less to avoid false correlations. (This requirement can be relaxed somewhat by utilizing the confidence ellipses, as discussed in Section VI-B.) It should be noted that when the fault timing is accurate to a few milliseconds, somewhat larger average errors can be tolerated in the lightning location. When analyzing distribution lines and when the line separation is of the order of one kilometer or less, then location errors as small as a few hundred meters can cause confusion and limit inferences about the causes and effects of individual faults.

C. Lightning Event Timing

The accuracy required for the flash or stroke times also depends on the application. A flash timing accuracy of a few seconds is usually more than adequate for storm tracking and measurements of flash densities. Flash timing to about a second is normally required to correlate a specific CG flash with a power outage or interruption. Finally, if one wishes to identify the specific return stroke that caused a fault, then the times of both the stroke and the fault must be known to a few milliseconds. We have seen that the NLDN stroke times are now accurate to a few microseconds due to the use of GPS timing in the sensors and the NLDN optimization algorithm. Older networks that do not use satellite-based clocks can have timing errors of seconds to minutes.

D. Peak Current Estimates

In Section IV-F, we noted that there is an inherent uncertainty of at least 20–30% in the NLDN estimates of the peak stroke current, even when sensor calibration and propagation effects have been addressed. The primary applications of these estimates by power utilities are in designing and evaluating lightning protection systems. For example, a cumulative distribution of peak currents provides the source data set for computing the theoretical "risk" for faults on transmission and distribution lines and for estimating lightning damage to substations and other utility equipment. In such applications, an error in peak current of the order of 30% can usually be tolerated. Great care should be taken when employing peak current estimates from small uncalibrated networks.

E. Flash and Stroke Information

Lightning "flash" reports typically contain the location and peak current of the first return stroke and a count of all strokes

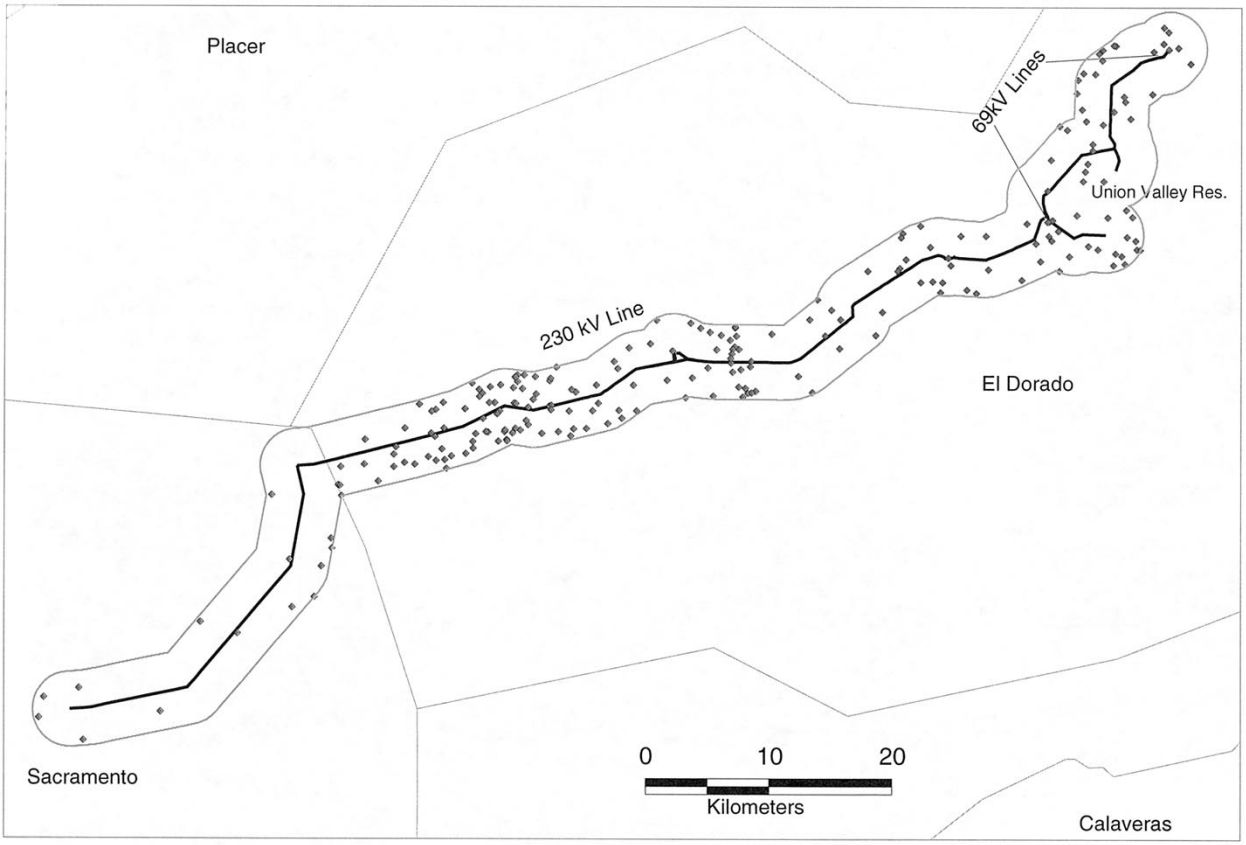

Fig. 13. The SMUD transmission line and an "asset exposure map" that shows all lightning strikes within 3.0 km of the line in bold.

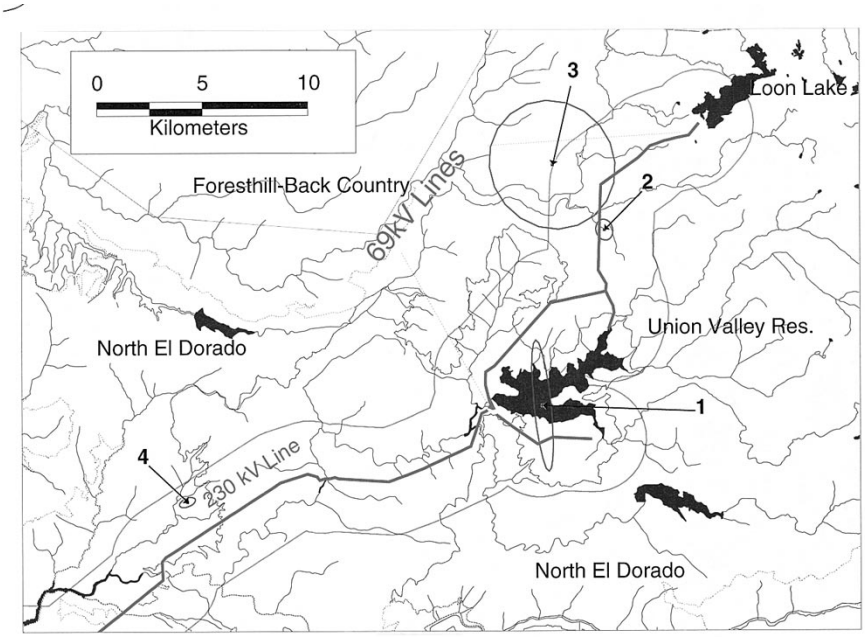

Fig. 14. Four strokes (out of 24) that were time correlated with faults and the associated 50% confidence regions. Strokes 1–3 were near 69-kV lines and stroke 4 was near a 230-kV line.

(multiplicity). NLDN "flash counts" are available for many years and are a quantitative replacement for the thunderday or thunderhour estimates of lightning exposure. From a power utility perspective, these flash data are also adequate for real-time thunderstorm warnings and estimating differences in lightning exposure in different geographic regions. However,

in order to fully assess the lightning threat to a specific utility asset, the data on all return strokes, including multiple ground contacts, need to be considered. Hence, for a complete evaluation of the threat from CG lightning, one should use the area density of strike points and include the distributions of the peak currents, the interstroke intervals, and the multiplicity of strokes at the different points. At the moment, the NLDN is limited in that it can resolve only strike points that are separated by at least 300–400 m. In order to obtain better information, it will first be necessary to locate individual strokes to very high accuracy, and then to group the strokes appropriately into the different strike points and flashes. On average, the NLDN today resolves about 1.3–1.4 strike points for each CG flash.

From the practical point of view, the methods that are used to group strokes into flashes do affect interpretations of the data. As noted in Section IV-E, a direction-based flash-grouping algorithm tends to overestimate the flash multiplicity and a location-based method tend to produce multiplicities that depend on the network detection efficiency. (This issue is discussed in more detail in [47].) Therefore, it is very important to understand the spatial resolution of the measuring network and the parameters that are used to group strokes into flashes. In particular, the clustering range and the maximum duration of a flash strongly affect the flash counts and the multiplicity distributions.

VIII. Conclusions and Future Directions

We have described the U.S. NLDN—the first lightning detection network to operate in real time on a continental scale. The NLDN detects and locates each return stroke in each CG flash that exceeds a nominal peak current. We have discussed the salient performance parameters of this network and some of the practical limitations in lightning detection. We have also described several applications of NLDN data by electric power utilities and how these applications are affected by network performance.

In the future, the NLDN sensors and data processing algorithms will be improved so as to obtain better location accuracy and detection efficiency. As time and resources permit, the NLDN will also attempt to obtain additional information that is relevant to the design and assessment of lightning protection by electric utilities. More specifically, research efforts will be directed toward estimating the impulse charge in each return stroke and estimating the rate of rise of current, at least to the extent that such an estimate is possible given the constraints imposed by radio propagation.

Acknowledgment

The authors would like to thank M. Sanderson Rae and Y. Banegas for their assistance in preparing this manuscript.

References

[1] M. A. Uman, *Lightning*. New York: McGraw-Hill, 1969; reprinted with supplement, New York: Dover, 1984.
[2] ——, *The Lightning Discharge*. Orlando, FL: Academic, 1987.
[3] M. A. Uman and E. P. Krider, "A review of natural lightning: Experimental data and modeling," *IEEE Trans. Electromagn. Compat.*, vol. EMC-24, pp. 79–112, May 1982.
[4] ——, "Natural and artificially initiated lightning," *Sci.*, vol. 246, pp. 457–464, 1989.
[5] K. Berger, R. B. Anderson, and H. Kroninger, "Parameters of lightning flashes," *Electra*, vol. 41, pp. 23–37, 1975.
[6] E. Garbagnati and G. B. L. Piparo, "Parameter von Blitzströmen," *Electrotech. Z. etz-a*, vol. 103, pp. 61–65, 1982.
[7] R. J. Fisher, G. H. Schnetzer, R. Thottappillil, V. A. Rakov, M. A. Uman, and J. D. Goldberg, "Parameters of triggered-lightning flashes in Florida and Alabama," *J. Geophys. Res.*, vol. 98, pp. 22 887–22 902, 1993.
[8] E. P. Krider, C. Leteinturier, and J. C. Willett, "Submicrosecond fields radiated during the onset of first return strokes in cloud-to-ground lightning," *J. Geophys. Res.*, vol. 101, pp. 1589–1597, 1996.
[9] J. C. Willett, E. P. Krider, and C. Leteinturier, "Submicrosecond field variations during the onset of first return strokes in cloud-to-ground lightning," *J. Geophys. Res.*, vol. 103, pp. 9027–9034, 1998.
[10] C. D. Weidman and E. P. Krider, "The fine structure of lightning return stroke waveforms," *J. Geophys. Res.*, vol. 83, pp. 6239–6247, 1978; correction, *J. Geophys. Res.*, vol. 87, p. 7351, 1982.
[11] W. H. Beasley, M. A. Uman, and P. L. Rustan, "Electric fields preceding cloud-to-ground lightning flashes," *J. Geophys. Res.*, vol. 87, pp. 4883–4902, 1982.
[12] E. P. Krider, C. D. Weidman, and R. C. Noggle, "The electric fields produced by lightning stepped leaders," *J. Geophys. Res.*, vol. 82, pp. 951–960, 1977.
[13] F. Horner, "Radio noise from thunderstorms," in *Advances in Radio Research*, J. A. Saxton, Ed. New York: Academic, 1964, vol. 2, pp. 121–204.
[14] E. T. Pierce, "Atmospherics and radio noise," in *Lightning, Physics of Lightning*, R. H. Golde, Ed. New York: Academic, 1977, vol. 1, ch. 10, pp. 351–384.
[15] M. A. Uman, D. K. McLain, and E. P. Krider, "The electromagnetic radiation from a finite antenna," *Amer. J. Phys.*, vol. 43, pp. 33–38, 1975.
[16] M. A. Uman, "Lightning return stroke electric and magnetic fields," *J. Geophys. Res.*, vol. 90, pp. 6121–6130, 1985.
[17] C. A. Nucci, G. Diendorfer, M. A. Uman, F. Rachidi, M. Ianoz, and C. Mazzetti, "Lightning return stroke current models with specified channel-base current: A review and comparison," *J. Geophys. Res.*, vol. 95, pp. 20 395–20 408, 1990.
[18] R. Thottappillil and M. A. Uman, "Comparison of lightning return-stroke models," *J. Geophys. Res.*, vol. 98, pp. 22 903–22 914, 1993.
[19] R. Thottappillil, V. A. Rakov, and M. A. Uman, "Distribution of charge along the lightning channel: Relation to remote electric and magnetic fields and to return-stroke models," *J. Geophys. Res.*, vol. 102, pp. 6987–7006, 1997.
[20] V. Rakov and M. A. Uman, "Review of lightning return stroke models," *IEEE Trans. Electromagn. Compat.*.
[21] D. M. Mach and W. D. Rust, "Two-dimensional velocity, optical risetime, and peak current estimates for natural positive lightning return strokes," *J. Geophys. Res.*, vol. 98, pp. 2635–2638, 1993.
[22] E. P. Krider, "On the electromagnetic fields, Poynting vector and peak power radiated by lightning return strokes," *J. Geophys. Res.*, vol. 97, pp. 15 913–15 917, 1992.
[23] H. Norinder, "Long-distance location of thunderstorms," in *Thunderstorm Electricity*, H. R. Byers, Ed. Chicago, IL: Univ. Chicago Press, 1953, ch. 14, pp. 276–327.
[24] R. A. Watson-Watt and J. F. Herd, "An instantaneous direct-reading radio goniometer," *J. Inst. Elect. Eng.*, vol. 64, pp. 611–622, 1926.
[25] R. A. Watson-Watt, J. F. Herd, and L. H. Bainbridge-Bell, *Applications of the Cathode Ray Oscillograph in Radio Research*. London, U.K.: His Majesty's Stationery Office, 1933.
[26] E. P. Krider, R. C. Noggle, and M. A. Uman, "A gated wideband magnetic direction-finder for lightning return strokes," *J. Appl. Meteor.*, vol. 15, pp. 301–306, 1976.
[27] E. P. Krider, R. C. Noggle, A. E. Pifer, and D. L. Vance, "Lightning direction finding systems for forest fire detection," *Bull. Amer. Meteor. Soc.*, vol. 61, pp. 980–986, 1980.
[28] E. A. Lewis, R. B. Harvey, and J. E. Rasmussen, "Hyperbolic direction finding with sferics of transatlantic origin," *J. Geophys. Res.*, vol. 65, pp. 1879–1905, 1960.
[29] A. C. L. Lee, "Ground truth confirmation and theoretical limits of an experimental VLF arrival time difference lightning flash locating system," *Quart J. Royal Meteor. Soc.*, vol. 115, pp. 1147–1166, 1989.

[30] P. W. Casper and R. B. Bent, "Results from the LPATS USA national lightning detection and tracking system for the 1991 lightning season," in *Proc. 21st Int. Conf. Lightning Protection*, Berlin, Germany, Sept. 1992, pp. 339–342.
[31] R. S. Bent and W. A. Lyons, "Theoretical evaluations and initial operational experiences of LPATS (Lightning Position and Tracking System) to monitor lightning ground strikes using a time-of-arrival (TOA) technique," in *7th Int. Conf. Atmospher. Electricity*, Albany, NY, June 1984, pp. 317–324 (preprints).
[32] R. L. Holle and R. E. López, "Overview of real-time lightning detection systems and their meteorological uses," NOAA Tech. Memo. ERL NSSL-102, Nat. Severe Storm Lab., Norman, OK, 1993, p. 68.
[33] D. E. Proctor, "A hyperbolic system for obtaining VHF radio pictures of lightning," *J. Geophys. Res.*, vol. 76, pp. 1478–1489, 1971.
[34] ——, "VHF radio pictures of cloud flashes," *J. Geophys. Res.*, vol. 86, pp. 4041–4071, 1981.
[35] ——, "Lightning and precipitation in a small multicellular thunderstorm," *J. Geophys. Res.*, vol. 88, pp. 5421–5440, 1983.
[36] D. E. Proctor, R. Uytenbogaardt, and B. M. Meredith, "VHF radio pictures of lightning flashes to ground," *J. Geophys. Res.*, vol. 93, pp. 12 683–12 727, 1988.
[37] C. Lennon and L. Maier, "Lightning mapping system," in *Proc. Int. Aerosp. Ground Conf. Lightning Static Electricity*, Cocoa Beach, FL, Apr. 1991, NASA Conf. Pub. 3106, vol. II, pp. 89-1–89-10.
[38] L. Maier, C. Lennon, T. Britt, and S. Schaefer, "Lightning detection and ranging (LDAR) system performance analysis," in *Proc. 6th Conf. Aviat. Weather Syst.*, Dallas, TX, Jan. 1995, Amer. Meteorol. Soc. Paper 8.9, p. 84.
[39] E. M. Thomson, P. J. Medelius, and S. Davis, "System for locating the sources of wideband dE/dt from lightning," *J. Geophys. Res.*, vol. 99, pp. 22 793–22 802, 1994.
[40] C. O. Hayenga and J. W. Warwick, "Two-dimensional interferometric positions of VHF lightning sources," *J. Geophys. Res.*, vol. 86, pp. 7451–7462, 1981.
[41] C. T. Rhodes, X.-M. Shao, P. R. Krehbiel, R. J. Thomas, and C. O. Hayenga, "Observations of lightning phenomena using radio interferometry," *J. Geophys. Res.*, vol. 99, pp. 13 059–13 082, 1994.
[42] X. M. Shao, P. R. Krehbiel, R. J. Thomas, and W. Rison, "Radio interferometric observations of cloud-to-ground lightning phenomena in Florida," *J. Geophys. Res.*, vol. 100, pp. 2749–2783, 1995.
[43] P. Richard, A. Soulage, P. Laroche, and J. Appel, "The SAFIR lightning monitoring and warning system: Application to aerospace activities," in *Proc. Int. Aerosp. Ground Conf. Lightning Static Electricity*, Oklahoma City, OK, Apr. 1988, pp. 383–390.
[44] P. Richard, A. Soulage, and F. Broutet, "The SAFIR lightning warning system," in *Proc. 1989 Int. Conf. Lightning Static Electricity*, Bath, U.K., Sept. 1989, pp. 2 B.1.1–2 B.1.5.
[45] P. Richard, "The SAFIR system: Early detection and alarm alert for risk of storms," in *Proc. Lightning Mountains*, Chamonix-Mont Blanc, France, June 1994, pp. 77–83.
[46] P. Richard and J. Y. Lojou, "Lightning and forecast of intense precipitation," in *Proc. Lightning Mountains*, Chamonix-Mont Blanc, France, June 1997, pp. 338–342.
[47] K. L. Cummins, M. J. Murphy, E. A. Bardo, W. L. Hiscox, R. B. Pyle, and A. E. Pifer, "A combined TOA/MDF technology upgrade of the U.S. National Lightning Detection Network," *J. Geophys. Res.*, vol. 103, pp. 9035–9044, 1998.
[48] D. M. Mach, D. R. MacGorman, W. D. Rust, and R. T. Arnold, "Site errors and detection efficiency in a magnetic direction-finder network for locating lightning strikes to ground," *J. Atmos. Ocean. Tech.*, vol. 3, pp. 67–74, 1986.
[49] R. E. Orville, R. W. Henderson, and L. F. Bosart, "An east coast lightning detection network," *Bull. Amer. Meteorol. Soc.*, vol. 64, pp. 1029–1037, 1983.
[50] R. E. Orville and H. Songster, "The east coast lightning detection network," *IEEE Trans. Power Delivery*, vol. PD-2, pp. 899–904, July 1987.
[51] R. E. Orville, "Lightning ground flash density in the contiguous United States—1989," *Monthly Weather Rev.*, vol. 119, pp. 573–577, 1990.
[52] R. E. Orville, R. W. Henderson, and R. B. Pyle, "The National Lightning Detection Network—Severe storm observations," in *Proc., 16th Conf. Severe Local Storms*, Kananaskis Park, AB, Canada, Oct. 1990, pp. J27–J30.
[53] W. A. Lyons, D. A. Moon, J. S. Schuh, N. J. Petit, and J. R. Eastman, "The design and operation of a national lightning detection network using time-of-arrival technology," in *Int. Conf. Lightning Static Electricity*, Bath, U.K, Sept. 1989, pp. 28-2.1–28-2.8.
[54] W. L. Hiscox, E. P. Krider, A. E. Pifer, and M. A. Uman, "A systematic method for identifying and correcting site errors in a network of magnetic direction finders," in *Proc. Int. Aerosp Ground Conf. Lightning Static Electricity*, Orlando, FL, 1984.
[55] R. M. Passi and R. E. López, "A parametric estimation of systematic errors in networks of magnetic direction finders," *J. Geophys. Res.*, vol. 94, pp. 13 319–13 328, 1989.
[56] K. L. Cummins, R. O. Burnett, W. L. Hiscox, and A. E. Pifer, "Line reliability and fault analysis using the National Lightning Detection Network," in *Proc. Precise Measurements Power Conf.*, Arlington, VA, Oct. 1993, pp. II-4.1–II-4.15.
[57] V. P. Idone, A. B. Saljoughy, R. W. Henderson, P. K. Moore, and R. B. Pyle, "A reexamination of the peak current calibration of the National Lightning Detection Network," *J. Geophys. Res.*, vol. 98, pp. 18 323–18 332, 1993.
[58] J. C. Willett, V. P. Idone, R. E. Orville, C. Leteinturier, A. Eybert-Berard, L. Barret, and E. P. Krider, "An experimental test of the 'transmission-line model' of electromagnetic radiation from triggered lightning return strokes," *J. Geophys. Res.*, vol. 93, pp. 3867–3878, 1988.
[59] R. E. López, R. L. Holle, R. Ortiz, and A. I. Watson, "Detection efficiency losses of networks of direction finders due to flash signal attenuation with range," in *Proc. Int. Aerosp. Ground Conf. Lightning Static Electricity*, Atlantic City, NJ, Oct. 1992, pp. 75-1–75-18 (FAA Report DOT/FAA/CT-92/20. Available through Nat. Tech. Inform. Service, Springfield, VA 22161).
[60] V. P. Idone, D. A. Davis, P. K. Moore, Y. Wang, R. W. Henderson, M. Ries, and P. F. Jamason, "Performance evaluation of the National Lightning Detection Network in the vicinity of Albany, New York: Part I—Detection efficiency," *J. Geophys. Res.*, vol. 103, pt. a, pp. 9045–9055, 1998.
[61] R. G. Stansfield, "Statistical theory of DF fixing," *J. Inst. Elect. Eng.*, vol. 94, pp. 762–770, 1947.
[62] V. P. Idone, D. A. Davis, P. K. Moore, Y. Wang, R. W. Henderson, M. Ries, and P. F. Jamason, "Performance evaluation of the National Lightning Detection Network in the vicinity of Albany, NY: Part II—Location accuracy," *J. Geophys. Res.*, vol. 103, pt. b, pp. 9057–9069, 1998.
[63] B. Fischer and E. P. Krider, "'On-line' lightning maps lead crews to 'trouble'," *Elect. World*, vol. 196, 1982.
[64] V. P. Idone and R. E. Orville, "Delimiting 'thunderstorm watch' periods by real-time lightning location for a power utility company," *Weather Forecasting*, vol. 5, pp. 141–147, 1990.
[65] T. Maffetone, D, Mark, W. Montgomery, and R. Noberini, "More accurate lightning data reduce utility's thunderstorm watch periods," *Elect. Power Res. Inst. Innovator*, Sept. 1991 (IN-100026, available from EPRI, Palo Alto, CA 94303).
[66] G. Bowden and R. N. Keener, Jr., "Duke power uses lightning network to reduce crew dispatch costs," *Elect. Power Res. Inst. Innovator*, Palo Alto, CA 94303, Dec. 1993 IN-101090, available from EPRI, Palo Alto, CA 94303).
[67] R. Bernstein, R. Samm, K. Cummins, R. Pyle, and J. Tuel, "Lightning detection network averts damage and speeds restoration," in *Proc. IEEE Comput. Applicat. Power*, Apr. 1996, vol. 9, pp. 12–17.
[68] M. W. Marshall and B. P. Angeli, "Establishing a lightning protection evaluation program for distribution and subtransmission lines," *IEEE Ind. Applicat. Mag.*, vol. 4, pp. 18–24, May/June 1998.
[69] S. A. Prentice, "Frequency of lightning discharges," in *Lightning, Physics of Lightning*, R. H. Golde, Ed. New York: Academic, 1977, vol. 1, p. 7.
[70] CIGRE, Document TF33.01.02, *Lightning Locating Systems*, Draft no. 3, Aug. 1997.
[71] L. Byerley III, G. K. L. Cummins, J. Tuel, D. J. Hagberg Jr., and W. Bush, "The measurement and use of lightning ground flash density," in *Proc. Int. Aerosp. Ground Conf. Lightning Static Electricity*, Williamsburg, VA, Sept. 1995, pp. 61-1–61-13.
[72] R. E. López, R. L. Holle, A. I. Watson, and J. Skindlov, "Spatial and temporal distributions of lightning over Arizona from a power utility perspective," *J. Appl. Meteorol.*, vol. 36, pp. 825–831, 1997.
[73] "Lightning protection design workstation," Tech. Rep. TR-000530, Electric Power Res. Inst., Menlo Park, CA, 1992.
[74] D. L. Van House, K. L. Cummins, and J. V. Tuel, "Applications of the U.S. National Lightning Detection Network in line reliability and fault analysis," in *Proc. CIGRE Int. Workshop Line Surge Arresters Lightning*, Rio de Janeiro, Brazil, Apr. 1996.
[75] J. G. Kappenman and D. L. Van House, "Location-centered mitigation of lightning-caused disturbances," in *Proc. IEEE Comput. Applicat. Power*, July 1996, pp. 36–40.

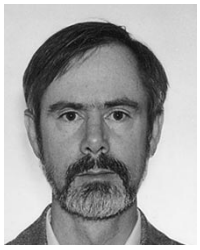

Kenneth L. Cummins received the B.S. degree in electrical engineering from the University of California, Irvine, in 1973 and the M.S. and Ph.D. degrees in electrical engineering from Stanford University, Stanford, CA, in 1974 and 1978, respectively.

He is currently the Vice President of Engineering for Global Atmospherics, Inc., Tucson, AZ. In addition to his management responsibilities, he continues to contribute technically and scientifically in the fields of atmospheric physics, instrumentation, modeling, and signal processing. He is the author of over 40 scientific papers and holds five U.S. patents.

E. Philip Krider received the B.A. degree in physics from Carleton College, Northfield, MN, in 1962, and the M.S. and Ph.D. degrees in physics from the University of Arizona, Tucson, in 1964 and 1969, respectively.

He is a Professor in the Institute of Atmospheric Physics and Department of Atmospheric Sciences, University of Arizona, where he teaches and conducts research on the physics of lightning, thundercloud electricity, lightning detection, lightning protection, and other problems in atmospheric electricity. He is the author of over 120 scientific papers and eight patents. He is a former Cochief editor and editor of the *Journal of Atmospheric Sciences* and an associate editor of the *Journal of Geophysical Research*.

Dr. Krider is a Fellow of the American Geophysical Union and the American Meteorological Society (AMS) and in 1985 he received the AMS Award for Outstanding Contribution to the Advance of Applied Meteorology. He is currently President of the International Commission on Atmospheric Electricity.

Mark D. Malone (M'96) received the B.A. (*cum laude*) degree in geography from the State University of New York at Albany, in 1989.

He is the Electric Utility Industry Manager at Global Atmospherics, Inc., Tucson, AZ. He continues to contribute to the Electric Utility's understanding of lightning, utilizing a geographic information system approach.

Mr. Malone is a member of the International Geographical Honor Society and the American Meteorological Society.